Stem Cell Reports
Article

ISSCR

OPEN ACCESS

In Vivo Maturation of Human Induced Pluripotent Stem Cell-Derived Cardiomyocytes in Neonatal and Adult Rat Hearts

Shin Kadota,[1,2,3] Lil Pabon,[1,2,3] Hans Reinecke,[1,2,3] and Charles E. Murry[1,2,3,4,5,*]
[1]Department of Pathology, University of Washington, 850 Republican Street, Brotman Building Room 453, Seattle, WA 98109, USA
[2]Institute for Stem Cell and Regenerative Medicine
[3]Center for Cardiovascular Biology
[4]Department of Bioengineering
[5]Department of Medicine/Cardiology
University of Washington, Seattle, WA 98109, USA
*Correspondence: murry@uw.edu
http://dx.doi.org/10.1016/j.stemcr.2016.10.009

SUMMARY

We hypothesized that the neonatal rat heart would bring transplanted human induced pluripotent stem cell-derived cardiomyocytes (hiPSC-CMs) to maturity as it grows to adult size. In neonatal rat heart, engrafted hiPSC derivatives developed partially matured myofibrils after 3 months, with increasing cell size and sarcomere length. There was no difference between grafts from hiPSC-CMs or hiPSC-derived cardiac progenitors (hiPSC-CPs) at 3 months, nor was maturation influenced by infarction. Interestingly, the infarcted adult heart induced greater human cardiomyocyte hypertrophy and induction of cardiac troponin I expression than the neonatal heart. Although human cardiomyocytes at all time points were significantly smaller than the host rat cardiomyocytes, transplanted neonatal rat cardiomyocytes reached adult size and structure by 3 months. Thus, the adult rat heart induces faster maturation than the neonatal heart, and human cardiomyocytes mature more slowly than rat cardiomyocytes. The slower maturation of human cardiomyocytes could be related to environmental mismatch or cell-autonomous factors.

INTRODUCTION

Human pluripotent stem cell-derived cardiomyocytes (hPSC-CMs) are promising candidates for cell therapy for injured and failing hearts due to their unlimited availability and potential for remuscularization (Chong et al., 2014; Laflamme and Murry, 2011; Shiba et al., 2016). However, differentiated cardiomyocytes have a fetal phenotype in structure and function, including small cell size, absence of transverse tubules (T tubules), persistent automaticity, metabolic dependence on glycolysis, lack of inotropic response to adrenergic stimulation, and so forth (Yang et al., 2014a; Zhu et al., 2014). This immature phenotype is one of the hurdles to overcome for clinical applications, modeling late-onset diseases, and accurate drug testing. Several methods to enhance maturation of hPSC-CMs in vitro have been developed, including long-term culture (Denning et al., 2016; Kamakura et al., 2013; Lundy et al., 2013), electrical stimulation (Nunes et al., 2013), mechanical loading (Tulloch et al., 2011), structural cues (Carson et al., 2016), culture substrate (Feaster et al., 2015), microRNA transfection (Kuppusamy et al., 2015), and chemical treatments (Yang et al., 2014b). At present, however, none of these stimuli is sufficient to induce complete maturation equivalent to adult cardiomyocytes.

On the other hand, substantial maturation of hPSC-CMs has been observed after in vivo cell transplantation into various adult animals, including mice (Funakoshi et al., 2016), rats (Caspi et al., 2007; Laflamme et al., 2005), and non-human primates (Chong et al., 2014). Hearts in living animals may have various effects, including mechanical, electric, and biochemical cues to enhance maturation of injected human cells beyond species differences. In this study we tested the hypothesis that the neonatal rat heart, by virtue of its rapid postnatal growth and maturation, would induce accelerated maturation of hPSC-CMs. There is some support for this notion, in that the growing rat brain enhances maturation of human neural progenitors after cell transplantation (Englund et al., 2002). Because neonatal hearts have recently been shown to have regenerative capacity after apical resection (Porrello et al., 2011) and myocardial infarction (MI) (Porrello et al., 2013), we also explored the behavior of hPSC-CMs transplanted into infarcted versus healthy neonatal myocardium. We report that although significant maturation of hPSC-CMs occurs in neonatal hearts, even greater maturation occurs in adult hearts, and that neonatal heart regeneration does not influence the extent of maturation.

RESULTS

hiPSC-CM Transplantation to Uninjured Neonatal Rat Hearts

At the starting point (18–20 days after induction of differentiation [Figure S1A]), 80.7% ± 4.9% (from 66% to 87%) of cells were cardiac troponin T (cTNT)-positive by flow cytometry (Figure S1B). Although undifferentiated human

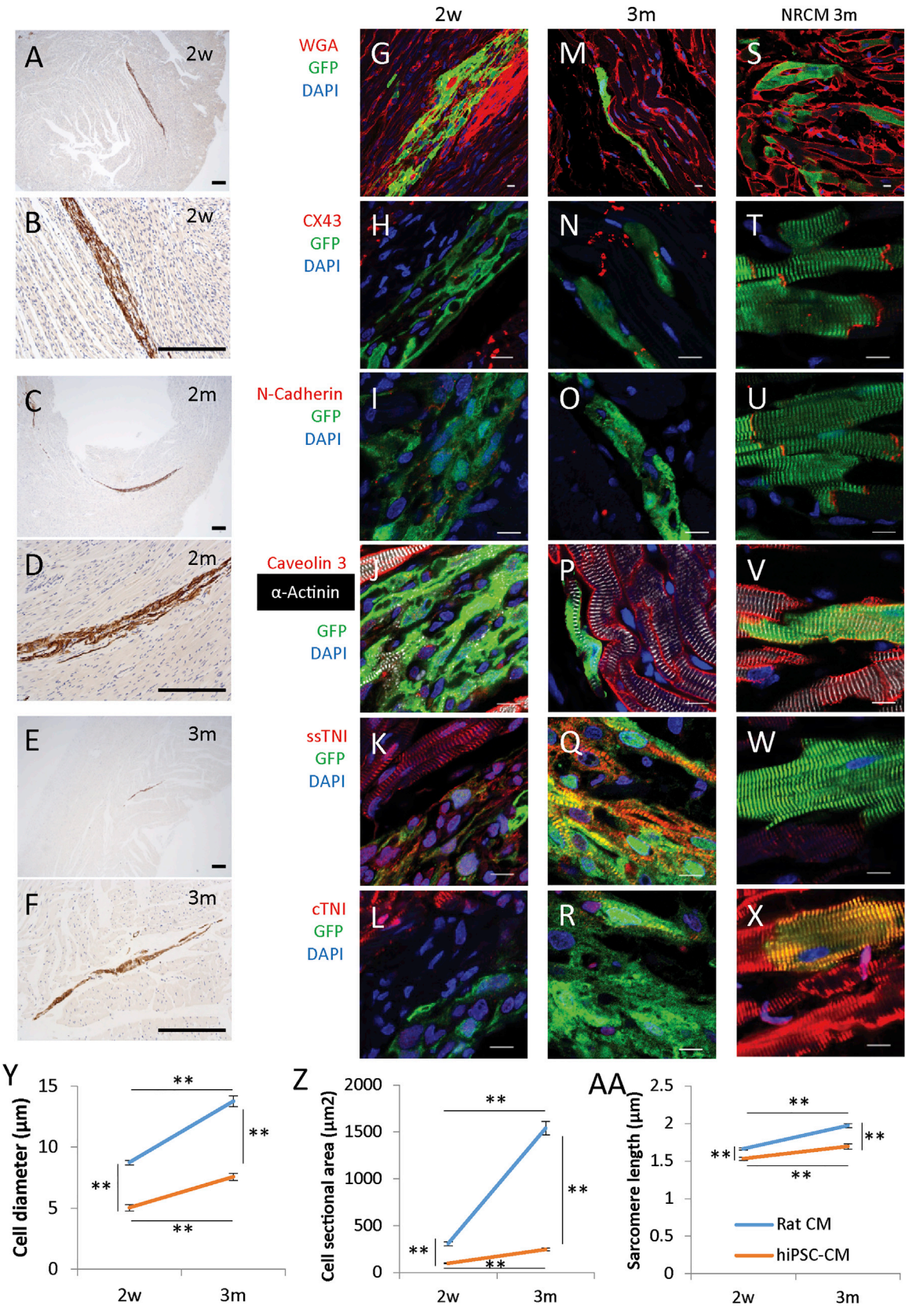

(legend on next page)

induced PSCs (hiPSCs) were genetically engineered to integrate GCaMP3 by zinc finger endonuclease and subsequently cloned, we observed some epigenetic silencing of the transgene, with 45.2% ± 12.6% (from 32% to 57%) of differentiated cells showing GCaMP3 fluorescence (Figure S1C). All morphometry was done on GFP-positive cells, but for histology images some graft cells may appear GFP negative due to this mosaicism (Figures 1Q, 1R, and 3G–3R).

We injected 2–5 × 10^5 hiPSC-CMs into uninjured hearts of athymic neonatal rats at 1–3 days after birth and tracked them by staining for the GFP epitope of GCaMP3 (Figures 1A–1F). Despite the limited volume that can be injected into the neonatal heart, injected cells survived from days 14–84 after cell injection. The GFP-positive graft area correlated well with staining for β-myosin heavy chain or human mitochondria antibodies (Figures S1E–S1G). From 2 weeks to 3 months, engrafted hiPSC-CMs enlarged from 97.4 ± 4.6 to 246.5 ± 15.1 μm^2 (wheat germ agglutinin [WGA] staining, Figures 1G and 1M), and developed gap junctions (connexin-43 staining, Figures 1H and 1N) and adherens junctions (N-cadherin staining, Figures 1I and 1O). Distributions of gap junctions and adherens junctions were circumferential to the hiPSC-CMs, although they polarize to the intercalated disk after 7 years and 1 year after birth, respectively, in human development (Vreeker et al., 2014). Grafted human cells also developed well-defined sarcomere structure (α-actinin staining), although there was no significant T-tubule formation in the graft (caveolin-3 staining, Figures 1J and 1P). Most cells express slow skeletal troponin I (ssTNI; Figures 1K and 1Q) but are negative for cardiac troponin I (cTNI; Figures 1L and 1R) at both day 14 and day 84 after cell transplantation. Cell diameter, cell area, and sarcomere length of hiPSC-CMs increased by 50.2%, 153%, and 10.6%, respectively, from day 14 to day 84 after cell injection. Despite these increases, mean cell diameter, cell area and sarcomere length of grafted hiPSC-CMs were significantly smaller than host rat cells both at 14 and 84 days after cell transplantation (Figures 1Y, 1Z, and 1AA).

We then compared hiPSC-CM maturation to that of GFP-labeled neonatal rat cardiomyocytes (NRCMs), grafted into uninjured neonatal rat hearts by the same procedure. In contrast to the human cardiomyocytes, the rat cells fully matured as the host cell after 3 months (Figures 1S–1X). Cell size (Figure 1S), polarized distributions of connexin-43 (Figure 1T) and N-cadherin (Figure 1U), sarcomere development and T-tubule formation (Figure 1V), and complete isoform switch from slow skeletal to cardiac troponin I (TNI) (Figures 1W and 1X) were all indistinguishable from the host rat cells after 3 months of NRCM transplantation. This indicates that complete graft maturation can occur within this environment, and that NRCMs mature much more quickly than hiPSC-CMs.

hiPSC-CM Transplantation in Infarcted Neonatal and Adult Rat Hearts

Next, we induced MI at days 1–3 after birth, and injected 2–5 × 10^5 hiPSC-CMs just after ligation of the left anterior descending artery (LAD). Non-viable area was 18.5% ± 4.5% of the left ventricle after 3 days of infarction by triphenyltetrazolium chloride (TTC) staining (n = 4, Figure S2). Scar size, detected by Masson trichrome staining (Figures 2A–2I and 3A), significantly decreased over time when it was normalized to left ventricle size (n = 4, Figure 2J); however, absolute volume of scar significantly increased over time (n = 4, Figure 2K) while the healthy ventricle grew around it.

Injected hiPSC-CMs engrafted and survived up to 3 months in the infarcted neonatal rat hearts (Figures 3B and 3C). We found that cell maturation was generally similar to that of the grafted cells in uninjured neonatal rats, including the increase in cell size (Figure 3G), circumferential distributions of gap junctions and adherens junctions (Figures 3H and 3I), partially matured sarcomere structure, absence of T tubules (Figure 3J), and abundant expression of ssTNI with limited detection of cTNI (Figures 3K and 3L). There was no significant difference in cell diameter, cell sectional area, and sarcomere length of engrafted hiPSC-CMs in uninjured and injured neonatal rat hearts (Figures S3A–S3C).

Next, we compared the maturation of hiPSC-CM grafts, 3 months after delivery to the infarcted neonatal versus infarcted adult rat hearts. Graft size was larger in the adult

Figure 1. In Vivo Maturation of hiPSC-CMs and Neonatal Rat CMs in Uninjured Growing Rat Hearts

(A–F) GFP staining of growing rat hearts at 14 days (A and B), 56 days (C and D), and 84 days (E and F) after hiPSC-CM injection.

(G–R) Magnified images of engrafted hiPSC-CMs at 14 days (2w; G–L) and 84 days (3m; M–R) after cell transplantation to neonates. Wheat germ agglutinin (WGA) is used to detect cell membranes, connexin-43 (CX43) is for gap junctions, N-cadherin is for adherence junction, caveolin-3 is for T tubules, α-actinin is for sarcomere, slow skeletal troponin I (ssTNI) is the fetal isoform of TNI, and cardiac TNI (cTNI) is for adult isoform of TNI.

(S–X) Magnified images of engrafted NRCMs at 84 days after cell transplantation to neonates. GFP-labeled NRCMs mature as host rat cells.

(Y–AA) Comparison of cell diameter (Y), cell sectional area (Z), and sarcomere length (AA) of host rat CMs (n = 34 per group) and hiPSC-CMs (n = 34–40 per group) at 14 days and 84 days after cell injection. At all time points, rat cells are significantly larger than hiPSC-CMs. Data are mean ± SEM. **p < 0.01 by t test.

Scale bars represent 200 μm (A–F) and 10 μm (G–X).

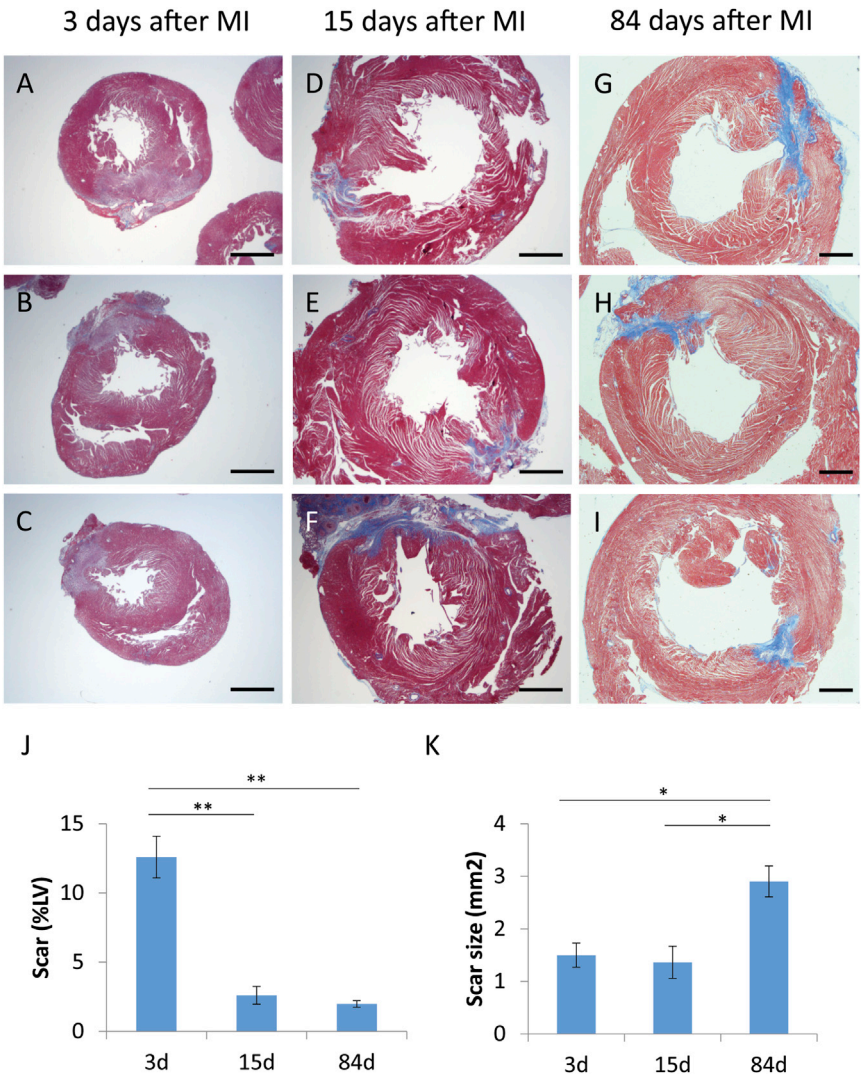

Figure 2. Myocardial Infarction in Neonatal Rat Hearts

(A–I) Masson trichrome staining of injured hearts at 3 (A–C), 15 (D–F), and 84 days (G–I) after MI. Scale bars, 1 mm.

(J) Scar size showing percentage of left ventricle (%LV) that significantly decreased over time (n = 4).

(K) Absolute scar size that significantly increased over time (n = 4).

Data are mean ± SEM. $^{**}p < 0.01$, $^{*}p < 0.05$ by ANOVA with Bonferroni's post hoc analysis.

(Figures 3D–3F) because injected cell numbers to adults were more than 20 times greater than could be delivered to neonates. Distributions of connexin-43 and N-cadherin were more polarized to the intercalated disk of hiPSC-CMs in adult infarcts (Figures 3N and 3O). Sarcomere development was similar in neonatal and adult infarcted systems, and no T-tubule formation in hiPSC-CMs was seen in either neonatal or adult hosts (Figures 3J and 3P). Expression of cTNI was noticeably greater in hiPSC-CMs engrafted in adults, compared with the minimal expression levels found in the grafts placed in neonates (Figures 3L and 3R). Mean grafted cell diameter and sarcomere length were similar (Figures 3S and 3U), but mean cell sectional area of hiPSC-CMs engrafted in injured neonates was significantly larger in hiPSC-CMs engrafted in adults (Figure 3T). Thus, contrary to our hypothesis, the adult heart promoted further maturation of hiPSC-CMs, evidenced by increased cell size, increased polarization of connexin-43 and N-cadherin, and isoform switching of TNI.

Cardiac Progenitor Cell Injection to Uninjured Neonatal Rat Hearts

Finally, we asked whether earlier-stage cardiac progenitor cells (hiPSC-CPs) might respond more to cues of the neonatal heart than definitive cardiomyocytes. To test this, we injected 2–5 × 10^5 hiPSC-CPs, obtained at day 5 after cardiac differentiation (Figure S1A), into the uninjured hearts of neonatal athymic rats. In day-5 differentiated hiPSC-CPs, pluripotent markers (*OCT4*, *SOX2*, and *NANOG*) were downregulated; however, genes related to cardiac mesodermal derivatives (*MESP1*, *KDR*, and *ISL1*) were highly upregulated, early cardiac development factors (*GATA4* and *TBX5*) were moderately upregulated, and cardiac makers (*NKX2.5* and *TNNT2*) were not expressed by

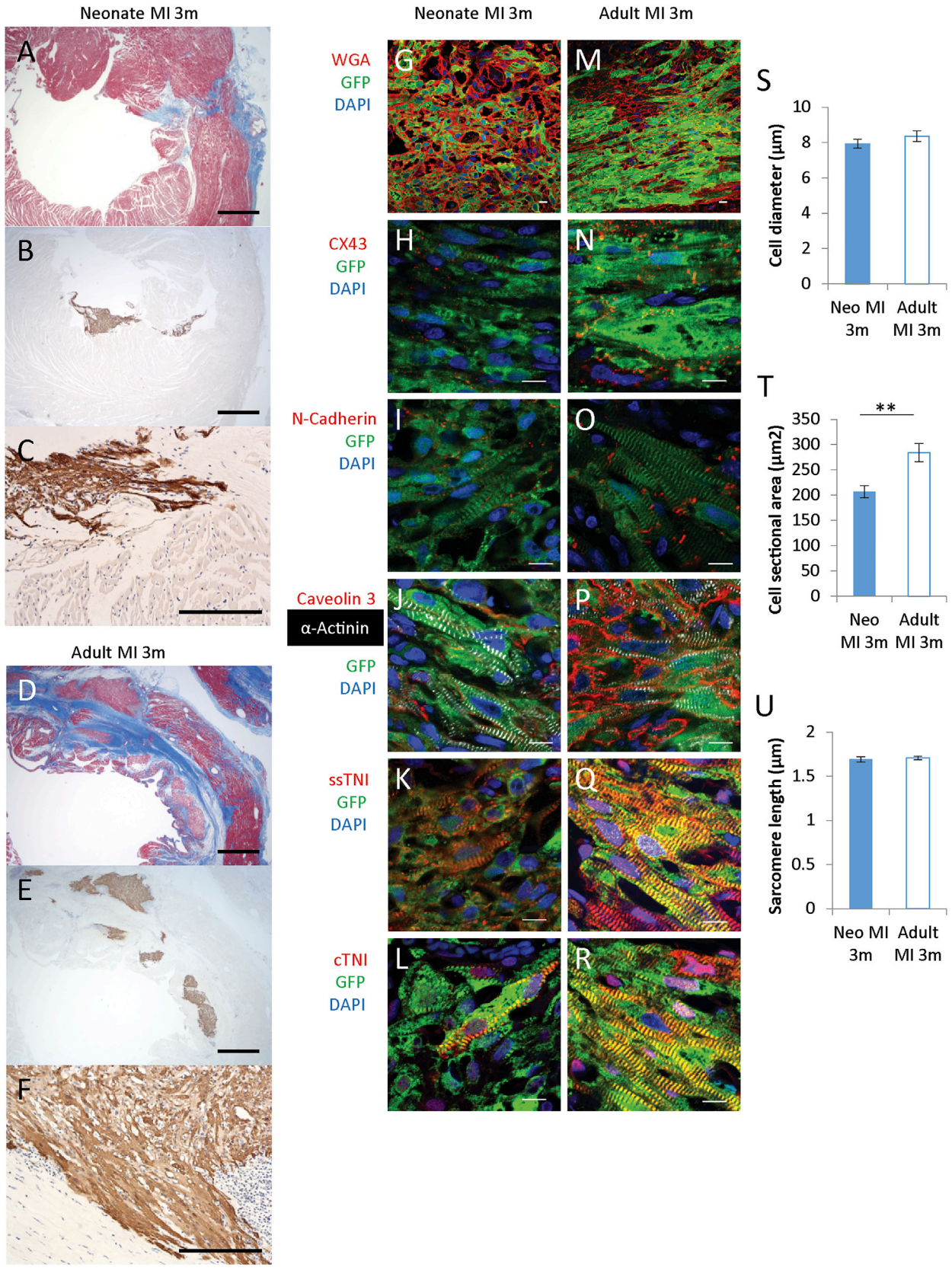

(legend on next page)

qRT-PCR (Figure S4). Although these progenitors did not yet express cTNT, parallel samples that were thawed and cultured in vitro yielded 82% cTNT-positive cells 10 days later. After transplantation, the hiPSC-CPs survived and differentiated to cardiomyocytes at 1 and 3 months after cell injection (Figures 4A–4D). Engrafted CMs in growing rat hearts were similar to hiPSC-CMs engrafted in adult injured rats, including the increase in cell size (Figure 4E), circumferential distributions of gap junctions (Figure 4F), polarized distribution of adherens junctions (Figure 4G), partially matured sarcomere structure, absence of T tubules (Figure 4H), and abundant expression of ssTNI with some detection of cTNI (Figures 4I and 4J). Interestingly, cell diameter of transplanted hiPSC-CPs after 3 months was larger than that of hiPSC-CMs (Figure 4K), but there was no difference in cell sectional area and sarcomere length (Figures 4L and 4M).

Among four different groups (hiPSC-CPs in neonate without MI, hiPSC-CMs in neonate without MI, hiPSC-CMs in neonate MI, and hiPSC-CMs in adult MI) at 3 months after cell transplantation as shown in Figure 5, there was no significant difference in cell diameter and sarcomere length (Figures 5A and 5B). However, cell sectional area of hiPSC-CMs in adult MI was significantly larger than that in neonatal MI (Figure 5C). Myofibril width measured at the Z band of hiPSC-CMs in adult MI was significantly thicker (3.99 μm) than in the others (2.42–3.10 μm; Figure 5D). All of the grafts at 3 months after cell injection were positive for ssTNI, indicating that none of the conditions resulted in its complete downregulation. Although there was minimal expression of cTNI in hiPSC-CM grafts placed in neonates, 38.3% of the graft area in infarcted adult hearts expressed cTNI. Surprisingly, 19.0% of the hiPSC-CP grafts placed in the neonatal heart expressed cTNI, significantly more than was seen with hiPSC-CM grafts (Figures 5E and S5). These data indicate that hiPSC-CPs develop mature sarcomere structure faster than hiPSC-CMs engrafted in neonatal rats, albeit slower than hiPSC-CMs engrafted in adult rats.

DISCUSSION

This study shows that hPSC-CMs can engraft in neonatal rat hearts up to 3 months, and investigates whether the in vivo postnatal developing environment can enhance maturation of hPSC-CMs. After 3 months of transplantation, engrafted cells were still smaller compared with the host rat cells, although they developed partially mature sarcomere structures. We also induced MI to the neonates, although there was no additional effect to enhance maturation of grafted human cells. Moreover, grafted hPSC derivatives in growing rat hearts were less mature than those in injured adult rat hearts. From these results, we conclude that the growing rat heart is not a particularly robust bioreactor to enhance maturation of hPSC-CMs.

In vitro cell culture conditions may arrest the maturation process of hPSC-CMs. For example, it was reported that hPSC-CMs cultured for more than 9 months were still immature, evidenced by the dominant fetal isoform of TNI: ssTNI (Bedada et al., 2014). In our previous non-human primate study (Chong et al., 2014), we observed that arrhythmias subsided as grafts matured. This is circumstantial evidence for immaturity contributing to arrhythmias. On the other hand, mature adult rat CMs did not survive after transplantation in adult rat hearts, although immature fetal and neonatal rat CMs survived (Reinecke et al., 1999). We will need additional studies to discover the optimal maturity of hPSC-CMs for clinical application.

One of the more striking findings from this study is the virtually complete structural maturation seen when NRCMs were transplanted to neonatal rat hearts. The rat cardiomyocytes underwent full physiological hypertrophy, formed T tubules and polarized intercalated disks, and expressed high levels of cTNI. Although engrafted hPSC-CMs showed significant maturation, they clearly were not at the adult stage even after 3 months in the rat heart. This difference could reflect an intrinsically slower maturation rate in the hiPSC-CMs or could be related to an imperfect match between the two species. In our non-human primate study, hPSC-CMs matured more than those engrafted in rat hearts measured by cell diameter (10.9 ± 2 μm versus 8.4 ± 0.3 μm). Although there are other differences between the studies (such as the use of human embryonic stem cell-CMs versus hiPSC-CMs and a 100-fold difference in cell dose), this difference in maturation supports the notion that closer species match gives greater maturity of engrafted hiPSC-CMs.

One possible reason of the difference between rat and human may be the discrepancy of maturity between

Figure 3. In Vivo Maturation of hiPSC-CMs in Injured Growing and Adult Rat Hearts at 3 Months after Cell Injection

(A–F) hiPSC-CM injection to neonatal rat MI (A–C) and hiPSC-CM injection to adult rat MI (D–F). Scar tissue is seen as blue by Masson trichrome staining (A and D) and grafts can be seen as brown by GFP staining (B, C, E, and F).

(G–R) Magnified images of engrafted hiPSC-CMs at 84 days of transplantation to injured neonatal rat (G–L) and injured adult rat (M–R). Scale bars represent 1 mm (A, B, D, and E), 200 μm (C and F), and 10 μm (G–R).

(S–U) Comparison of cell diameter (S), cell sectional area (T), and sarcomere length (U) of hiPSC-CMs (n = 40 per group) engrafted in injured neonatal rat and injured adult rat at 84 days after cell injection. Data are mean ± SEM. **p < 0.01 by t test.

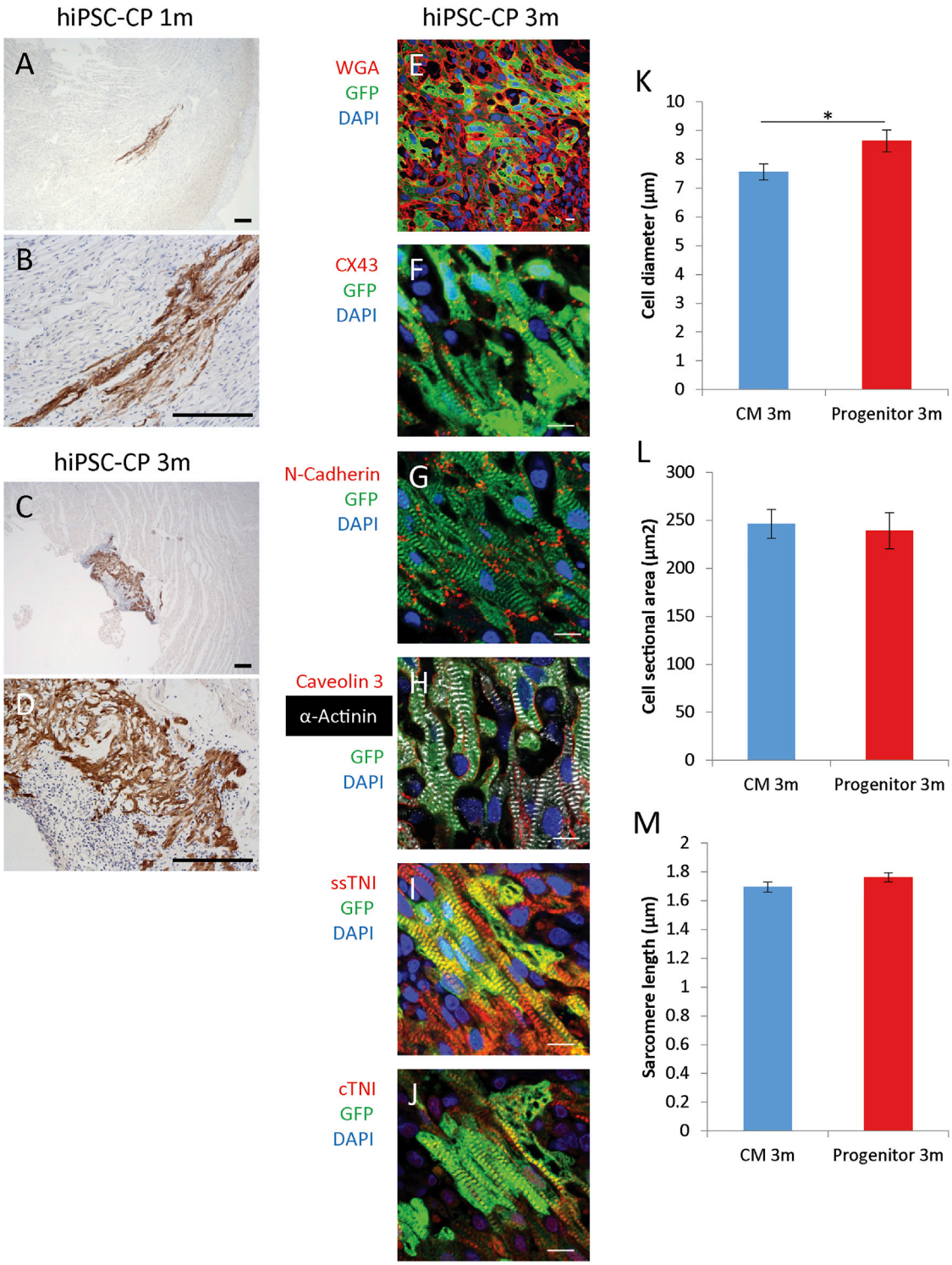

Figure 4. In Vivo Maturation of hiPSC-Derived Cardiac Progenitors in Uninjured Growing Rat Hearts

(A–D) GFP staining of growing rat hearts at 28 days (A and B) and 84 days (C and D) after hiPSC-CP injection. Scale bars, 200 μm.

(E–J) Magnified images of engrafted hiPSC-CPs at 84 days of transplantation to uninjured neonatal rats. Scale bars, 10 μm.

(K–M) Comparison of cell diameter (K), cell sectional area (L), and sarcomere length (M) of hiPSC-CMs and hiPSC-CPs (n = 40 per group) engrafted in injured neonatal rat at 84 days after cell injection. Data are mean ± SEM. *p < 0.05 by t test.

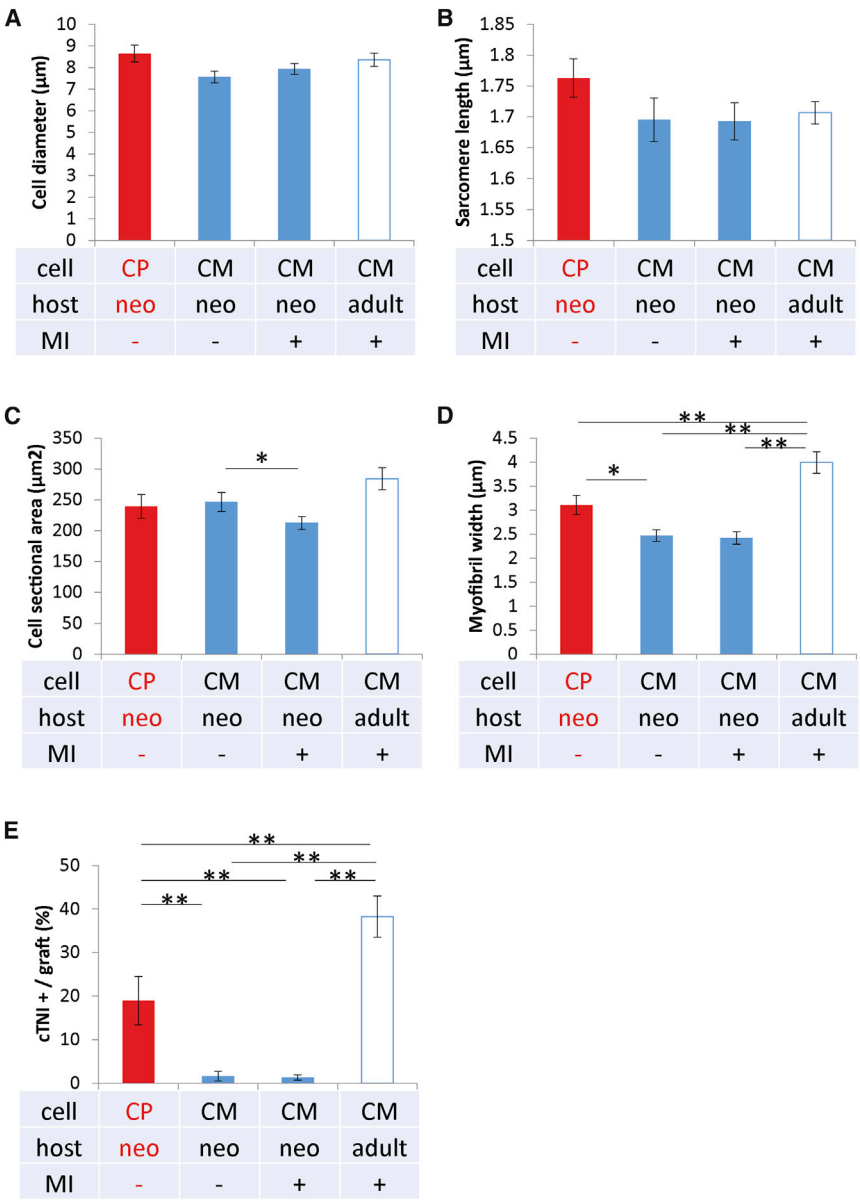

Figure 5. Comparison of hiPSC Derivatives Engrafted in Rat Hearts after 3 Months of Cell Transplantation

Cell diameter (A), sarcomere length (B), cell sectional area (C), and myofibril width (D) (n = 40 cells per group). (E) Percentage of cTNI-positive area in grafts (n = 4–5 images of grafts). CP, hiPSC-derived cardiac progenitors; CM, hiPSC-derived cardiomyocytes; neo, neonate. Data are mean ± SEM. $^{**}p < 0.01$, $^{*}p < 0.05$ by ANOVA with Bonferroni's post hoc analysis in (C) and (D), and by chi-square test in (E).

the two graft populations. At postnatal days 1–3, the neonatal rat heart is already expressing cTNI in transition of isoform switch, indicating that NRCMs are much more mature than hiPSC-CMs at 20 days of differentiation. Recently hPSC-CMs were shown to be equivalent to fetal heart during the first and second trimester by transcriptome analyses (van den Berg et al., 2015). If we could have injected hPSC-CMs to prenatal fetal rat hearts, the result might have been different. Another possibility is the differences of properties between rat and human cardiomyocytes, for example beating rate, Ca^{2+} handling, ion channels, and myofilament composition (Karakikes et al., 2015). These considerable differences may prevent maturation of hiPSC derivatives in rat hearts.

Finally, there was a possibility that definitive hiPSC-CMs at 20 days of differentiation have already lost the capacity to transform to fully mature cardiomyocytes in rat hearts. To test this, we transplanted mesodermal hiPSC-CPs to neonates. Engrafted hiPSC-CPs formed slightly larger cardiomyocytes with wider myofibrils and greater cTNI expression compared with hPSC-CMs after 3 months, supporting the notion that they have greater plasticity. On the other hand, they were less mature than engrafted hiPSC-CMs in adult rats. In other studies where cardiac progenitors were transplanted to adult mice or rats, there was no

significant difference in maturity between hPSC-CMs and progenitors, but the graft size of hPSC-CMs tended to be larger than that of cardiac progenitors (Fernandes et al., 2015; Funakoshi et al., 2016).

There are some limitations to this study. We observed greater induction of maturation of hiPSC-CMs in adult rat hearts than in neonatal rat hearts. However, we injected more than 20-fold hiPSC-CMs in adult rat hearts, because no grafts were detected in adult rats when we injected 5×10^5 cells in our previous study (Laflamme et al., 2005). Thus, there is a possibility that cell dose influenced the maturity of engrafted hiPSC-CMs after transplantation in the adult. Secondly, we observed discrepant maturation rates in human and rat cells. In principle, one explanation for the discrepant maturation rates could be the use of hiPSC-CMs for human cells and primary cardiomyocytes for rat cells. Transplanting human fetal cardiomyocytes or rat iPSC-CMs (Liao et al., 2009) could address this possibility. Thirdly, our study was largely observational. We need further studies, which are species-matched between host and graft, for example rat iPSC-CM transplant to rats versus monkey iPSC-CM transplant to monkey, to discover the full impact of species mismatch. Also, different species stem cell-derived CM transplantation to the same host can answer intrinsic "clock" differences.

In conclusion, in the growing rat hearts from neonate to adult, hiPSC-CPs and hiPSC-CMs matured partially; however, they were less mature than hiPSC-CMs engrafted in adult rat hearts. None of the human cells or host conditions reproduced rapid maturation of neonatal rat cardiomyocytes in the rat heart. Further study is necessary to determine the method to induce complete maturation of hPSC-CMs.

EXPERIMENTAL PROCEDURES

Cardiomyocyte Differentiation from Human Induced Pluripotent Stem Cells

All cardiomyocytes in this study were derived from 253G1 hiPSCs (Kyoto University), which were genetically engineered to express the Ca^{2+} indicator protein, GCaMP3, as described elsewhere (Chong et al., 2014; Shiba et al., 2012). Undifferentiated 253G1-GCaMP3 hiPSCs were maintained as described previously (Palpant et al., 2013). In brief, the hiPSCs were seeded on Matrigel-coated (BD Biosciences) plates and maintained with mouse embryonic fibroblast-conditioned medium (MEF-CM) containing 5 ng/mL human basic fibroblast growth factor (Peprotech; 100-18B) until appropriate confluency was observed. Directed differentiation of hiPSCs toward cardiomyocytes was performed in high-density monolayers, using a combination of 100 ng/mL activin A (R&D Systems), 5 ng/mL BMP4 (R&D Systems), 1 μM CHIR99021 (Cayman Chemicals), and 1 μM XAV939 (Tocris) as described previously (Hofsteen et al., 2016) and illustrated in Figure S1A.

Flow Cytometry

Cardiomyocyte purity was obtained by analyzing cTNT-positive cells using flow cytometry. Cells were fixed by paraformaldehyde and incubated with a mouse monoclonal cTNT antibody (Thermo Scientific; 1:100) or mouse immunoglobulin G1 K isotype control (eBioscience; 1:100), followed by incubation with an APC-conjugated goat anti-mouse secondary antibody. GCaMP3-positive cells were detected by fluorescein isothiocyanate without staining. Fluorescence characterization was performed on a BD FACS Canto II (BD Biosciences) and subsequently analyzed using FlowJo software. Only cultures having >66% cTNT-positive cells were used for hiPSC in vivo studies.

Cryopreservation and Cell Preparation for Transplantation

HiPSC-CPs and hiPSC-CMs used in this study were cryopreserved on days 5 and 18–20 of differentiation, respectively, and thawed immediately prior to cell injection, following our previously described protocol (Gerbin et al., 2015; Laflamme et al., 2007). One day prior to cryopreservation, cells were heat-shocked for 30 min at 42°C. Prior to enzymatic dispersion, the ROCK inhibitor Y-27632 (10 μM) was added to culture medium for 1 hr, and cells were dispersed by incubation with Versene followed by 0.05% trypsin in EDTA. HiPSC-CPs and hiPSC-CMs were resuspended in CryoStor cell preservation medium (C2874; Sigma) and frozen in cryovials in a controlled-rate freezer to −80°C before being stored in liquid nitrogen. To thaw cryopreserved cells, we thawed cryovials briefly at 37°C followed by addition of RPMI + B27 + insulin with Y-27632 (10 μM). Cells were washed with PBS and resuspended in an RPMI-based pro-survival cocktail (Laflamme et al., 2007) containing 50% growth factor-reduced Matrigel, 100 μM ZVAD (benzyloxycarbonyl-Val-Ala-Asp(O-methyl)-fluoromethyl ketone, Calbiochem), 50 nM Bcl-XL BH4 (cell-permeant TAT peptide, Calbiochem), 200 nM cyclosporine A (Novartis), 100 ng/mL insulin-like growth factor 1 (Peprotech), and 50 μM pinacidil (Sigma).

Animal Study

All animal procedures were conducted in accordance with the US NIH Policy on Humane Care and Use of Laboratory Animals, and protocols were reviewed in advance by the University of Washington Institutional Animal Care and Use Committee.

Cell Injection to Neonatal Rats

One to three days after birth, neonatal athymic rats (4–11 g, $Foxn1^{rnu}/Foxn1^{rnu}$) were anesthetized by isoflurane inhalation (0.5%–3%). As local analgesia, 4 mg/kg lidocaine and 2 mg/kg bupivacaine were given at the incision site. Lateral thoracotomy was performed by blunt dissection of intercostal muscles after skin incision. Then 2–5 μL of cell suspension containing $2–5 \times 10^5$ hiPSC-CMs or hiPSC-CPs was slowly injected into the anterior wall of left ventricle using a Hamilton syringe and a 29- or 30-gauge needle. In the indicated experiments, MI was induced by ligation of the mid-anterior wall of the left ventricle by 7-0 or 8-0 suture, just before cell injection. Chest and skin were closed by 6-0 sutures. Rats received analgesic (buprenorphine, 0.05 mg/kg) twice daily for 48 hr after surgery.

Neonatal Rat Cardiomyocyte Isolation and GFP Labeling

Neonatal rat hearts were harvested from 1-day-old athymic rats, minced, and digested three to four times for 15–30 min each, incubating at 37°C with a protease solution (0.1% collagenase type IV, 0.25% trypsin, 1 U/mL DNase I, 116 mM NaCl, 20 mM HEPES, 12.5 mM NaH_2PO_4, 5.6 mM glucose, 5.4 mM KCl, and 0.8 mM $MgSO_4$ [pH 7.35]). The isolated cells were collected by centrifugation and incubated on a 10-cm cell culture plate for 30 min at 37°C in a humidified incubator with 5% CO_2 air. Unattached cells were collected and seeded on laminin-coated 10-cm cell culture plates and were transfected overnight with an adenovirus carrying a cytomegalovirus promoter-EGFP transgene at an MOI of 500. The next day, GFP-transfected NRCMs were collected, suspended, in our pro-survival cocktail described above, and injected to uninjured neonatal rat hearts using the same protocol of hiPSC-CM injection. Cell preparations averaged 57% GFP-positive and 55% cTNT-positive.

Cell Injection to Adult Rats

The protocol for cell injection to adult rats has been detailed in multiple previous reports by our group (Fernandes et al., 2010; Gerbin et al., 2015; Laflamme et al., 2007). Eight- to ten-week-old male athymic rats (240–300 g) were anesthetized by intraperitoneal injection of 68.2 mg/kg ketamine and 4.4 mg/kg xylazine, intubated, and mechanically ventilated. A thoracotomy exposed the heart and LAD was occluded for 60 min and reperfused, and the chest was closed. Four days after ischemia/reperfusion injury, rats were anesthetized by isoflurane inhalation and mechanically ventilated. The heart was exposed via a second thoracotomy and 10×10^6 hiPSC-CMs were injected to the center of the infarcted left ventricle wall (three to four injections, 30 μL each). Chest and skin were closed by sutures and wound clips, respectively. Rats received analgesic (buprenorphine, 0.05 mg/kg) twice daily for 48 hr after each surgery. Cyclosporine A (5 mg/kg/day) was given for 7 days beginning the day before transplantation.

Immunohistochemical Analysis

Histological stains and subsequent analysis were conducted as described previously by our group (Chong et al., 2014; Gerbin et al., 2015; Laflamme et al., 2007). In brief, hearts were perfused with PBS and 150 mM KCl solution after harvesting, fixed overnight in 4% paraformaldehyde, sliced into 1- to 2-mm-thick sections, processed, sectioned, and stained with appropriate primary and secondary antibodies. Antibodies are listed in Table S1. Infarcts were visualized by Masson trichrome staining, and quantified by measuring scar area in three to five sections, normalized to the whole left ventricular area. For TTC staining, harvested hearts were stained without fixation and the percentage of viable (red) and non-viable (white) was quantified using ImageJ at 3 days after neonatal rat MI as described previously (Mahmoud et al., 2014). All immunofluorescent images were collected by a Nikon A1 Confocal System attached to a Nikon Ti-E inverted microscope platform. All images were collected as a single scan with the pinhole adjusted to 1 Airy unit at 1,024 × 1,024 pixel density. For figure preparation, images were processed to convert colors by Nikon NIS Elements software, if necessary. Sarcomere length and myofibril width were measured by α-actinin staining, and cell sectional area was measured by WGA staining using ImageJ.

qRT-PCR

Total RNA was isolated using the RNeasy Miniprep Kit (Qiagen), in accordance with the manufacturer's protocol including DNase treatment. First-strand cDNA from 500 ng of total RNA was synthesized using the SuperScript III Reverse Transcriptase Kit (Invitrogen). qRT-PCR was performed using SYBR Select Master Mix (Thermo Fisher) on a 7900HT fast real-time PCR system (Applied Biosystems). The copy number for each transcript is expressed relative to *GAPDH*. Primers are listed in Table S2.

Statistical Analysis

Statistical significance ($p < 0.05$) was detected by Student's t test (two-sided) or one-way ANOVA followed by Bonferroni's post hoc analysis. A chi-square test was used for comparisons of cTNI-positive area in grafts. All values are reported as means, and error bars in the figures represent SEM.

SUPPLEMENTAL INFORMATION

Supplemental Information includes five figures and two tables and can be found with this article online at http://dx.doi.org/10.1016/j.stemcr.2016.10.009.

AUTHOR CONTRIBUTIONS

S.K. and C.E.M. conceived and organized the project and wrote the manuscript; L.P. and H.R. contributed to experiments and data analysis.

ACKNOWLEDGMENTS

The authors thank Amy Martinson for surgery of adult rats, and Dr. Yuji Shiba at Shinshu University, Japan for providing 253G1-GCaMP3 hiPSCs. This work was supported by NIH grants P01 HL094374, R01 HL128362, R01 HL084642, U01 HL100405, and P01 GM081619, as well as an award from the Foundation Leducq Transatlantic Network of Excellence. We gratefully acknowledge funding support to S.K. from Banyu Life Science Foundation International and the American Heart Association (14POST20150045). C.E.M. is a scientific co-founder and equity holder in BEAT Biotherapeutics.

Received: August 25, 2016
Revised: October 28, 2016
Accepted: October 31, 2016
Published: January 5, 2017

REFERENCES

Bedada, F.B., Chan, S.S., Metzger, S.K., Zhang, L., Zhang, J., Garry, D.J., Kamp, T.J., Kyba, M., and Metzger, J.M. (2014). Acquisition of a quantitative, stoichiometrically conserved ratiometric marker of maturation status in stem cell-derived cardiac myocytes. Stem Cell Rep. *3*, 594–605.

Carson, D., Hnilova, M., Yang, X., Nemeth, C.L., Tsui, J.H., Smith, A.S., Jiao, A., Regnier, M., Murry, C.E., Tamerler, C., et al. (2016). Nanotopography-induced structural anisotropy and sarcomere development in human cardiomyocytes derived from induced pluripotent stem cells. ACS Appl. Mater. Inter. *8*, 21923–21932.

Caspi, O., Huber, I., Kehat, I., Habib, M., Arbel, G., Gepstein, A., Yankelson, L., Aronson, D., Beyar, R., and Gepstein, L. (2007). Transplantation of human embryonic stem cell-derived cardiomyocytes improves myocardial performance in infarcted rat hearts. J. Am. Coll. Cardiol. *50*, 1884–1893.

Chong, J.J., Yang, X., Don, C.W., Minami, E., Liu, Y.W., Weyers, J.J., Mahoney, W.M., Van Biber, B., Cook, S.M., Palpant, N.J., et al. (2014). Human embryonic-stem-cell-derived cardiomyocytes regenerate non-human primate hearts. Nature *510*, 273–277.

Denning, C., Borgdorff, V., Crutchley, J., Firth, K.S., George, V., Kalra, S., Kondrashov, A., Hoang, M.D., Mosqueira, D., Patel, A., et al. (2016). Cardiomyocytes from human pluripotent stem cells: from laboratory curiosity to industrial biomedical platform. Biochim. Biophys. Acta *1863*, 1728–1748.

Englund, U., Fricker-Gates, R.A., Lundberg, C., Bjorklund, A., and Wictorin, K. (2002). Transplantation of human neural progenitor cells into the neonatal rat brain: extensive migration and differentiation with long-distance axonal projections. Exp. Neurol. *173*, 1–21.

Feaster, T.K., Cadar, A.G., Wang, L., Williams, C.H., Chun, Y.W., Hempel, J.E., Bloodworth, N., Merryman, W.D., Lim, C.C., Wu, J.C., et al. (2015). Matrigel mattress: a method for the generation of single contracting human-induced pluripotent stem cell-derived cardiomyocytes. Circ. Res. *117*, 995–1000.

Fernandes, S., Naumova, A.V., Zhu, W.Z., Laflamme, M.A., Gold, J., and Murry, C.E. (2010). Human embryonic stem cell-derived cardiomyocytes engraft but do not alter cardiac remodeling after chronic infarction in rats. J. Mol. Cell Cardiol. *49*, 941–949.

Fernandes, S., Chong, J.J., Paige, S.L., Iwata, M., Torok-Storb, B., Keller, G., Reinecke, H., and Murry, C.E. (2015). Comparison of human embryonic stem cell-derived cardiomyocytes, cardiovascular progenitors, and bone marrow mononuclear cells for cardiac repair. Stem Cell Rep. *5*, 753–762.

Funakoshi, S., Miki, K., Takaki, T., Okubo, C., Hatani, T., Chonabayashi, K., Nishikawa, M., Takei, I., Oishi, A., Narita, M., et al. (2016). Enhanced engraftment, proliferation, and therapeutic potential in heart using optimized human iPSC-derived cardiomyocytes. Sci. Rep. *6*, 19111.

Gerbin, K.A., Yang, X., Murry, C.E., and Coulombe, K.L. (2015). Enhanced electrical integration of engineered human myocardium via intramyocardial versus epicardial delivery in infarcted rat hearts. PLoS One *10*, e0131446.

Hofsteen, P., Robitaille, A.M., Chapman, D.P., Moon, R.T., and Murry, C.E. (2016). Quantitative proteomics identify DAB2 as a cardiac developmental regulator that inhibits WNT/beta-catenin signaling. Proc. Natl. Acad. Sci. USA *113*, 1002–1007.

Kamakura, T., Makiyama, T., Sasaki, K., Yoshida, Y., Wuriyanghai, Y., Chen, J., Hattori, T., Ohno, S., Kita, T., Horie, M., et al. (2013). Ultrastructural maturation of human-induced pluripotent stem cell-derived cardiomyocytes in a long-term culture. Circ. J. *77*, 1307–1314.

Karakikes, I., Ameen, M., Termglinchan, V., and Wu, J.C. (2015). Human induced pluripotent stem cell-derived cardiomyocytes: insights into molecular, cellular, and functional phenotypes. Circ. Res. *117*, 80–88.

Kuppusamy, K.T., Jones, D.C., Sperber, H., Madan, A., Fischer, K.A., Rodriguez, M.L., Pabon, L., Zhu, W.Z., Tulloch, N.L., Yang, X., et al. (2015). Let-7 family of microRNA is required for maturation and adult-like metabolism in stem cell-derived cardiomyocytes. Proc. Natl. Acad. Sci. USA *112*, E2785–E2794.

Laflamme, M.A., and Murry, C.E. (2011). Heart regeneration. Nature *473*, 326–335.

Laflamme, M.A., Gold, J., Xu, C., Hassanipour, M., Rosler, E., Police, S., Muskheli, V., and Murry, C.E. (2005). Formation of human myocardium in the rat heart from human embryonic stem cells. Am. J. Pathol. *167*, 663–671.

Laflamme, M.A., Chen, K.Y., Naumova, A.V., Muskheli, V., Fugate, J.A., Dupras, S.K., Reinecke, H., Xu, C., Hassanipour, M., Police, S., et al. (2007). Cardiomyocytes derived from human embryonic stem cells in pro-survival factors enhance function of infarcted rat hearts. Nat. Biotechnol. *25*, 1015–1024.

Liao, J., Cui, C., Chen, S., Ren, J., Chen, J., Gao, Y., Li, H., Jia, N., Cheng, L., Xiao, H., et al. (2009). Generation of induced pluripotent stem cell lines from adult rat cells. Cell Stem Cell *4*, 11–15.

Lundy, S.D., Zhu, W.Z., Regnier, M., and Laflamme, M.A. (2013). Structural and functional maturation of cardiomyocytes derived from human pluripotent stem cells. Stem Cells Dev. *22*, 1991–2002.

Mahmoud, A.I., Porrello, E.R., Kimura, W., Olson, E.N., and Sadek, H.A. (2014). Surgical models for cardiac regeneration in neonatal mice. Nat. Protoc. *9*, 305–311.

Nunes, S.S., Miklas, J.W., Liu, J., Aschar-Sobbi, R., Xiao, Y., Zhang, B., Jiang, J., Masse, S., Gagliardi, M., Hsieh, A., et al. (2013). Biowire: a platform for maturation of human pluripotent stem cell-derived cardiomyocytes. Nat. Methods *10*, 781–787.

Palpant, N.J., Pabon, L., Rabinowitz, J.S., Hadland, B.K., Stoick-Cooper, C.L., Paige, S.L., Bernstein, I.D., Moon, R.T., and Murry, C.E. (2013). Transmembrane protein 88: a Wnt regulatory protein that specifies cardiomyocyte development. Development *140*, 3799–3808.

Porrello, E.R., Mahmoud, A.I., Simpson, E., Hill, J.A., Richardson, J.A., Olson, E.N., and Sadek, H.A. (2011). Transient regenerative potential of the neonatal mouse heart. Science *331*, 1078–1080.

Porrello, E.R., Mahmoud, A.I., Simpson, E., Johnson, B.A., Grinsfelder, D., Canseco, D., Mammen, P.P., Rothermel, B.A., Olson, E.N., and Sadek, H.A. (2013). Regulation of neonatal and adult mammalian heart regeneration by the miR-15 family. Proc. Natl. Acad. Sci. USA *110*, 187–192.

Reinecke, H., Zhang, M., Bartosek, T., and Murry, C.E. (1999). Survival, integration, and differentiation of cardiomyocyte grafts: a study in normal and injured rat hearts. Circulation *100*, 193–202.

Shiba, Y., Fernandes, S., Zhu, W.Z., Filice, D., Muskheli, V., Kim, J., Palpant, N.J., Gantz, J., Moyes, K.W., Reinecke, H., et al. (2012). Human ES-cell-derived cardiomyocytes electrically couple and suppress arrhythmias in injured hearts. Nature *489*, 322–325.

Shiba, Y., Gomibuchi, T., Seto, T., Wada, Y., Ichimura, H., Tanaka, Y., Ogasawara, T., Okada, K., Shiba, N., Sakamoto, K., et al. (2016). Allogeneic transplantation of iPS cell-derived cardiomyocytes regenerates primate hearts. Nature *538*, 388–391.

Tulloch, N.L., Muskheli, V., Razumova, M.V., Korte, F.S., Regnier, M., Hauch, K.D., Pabon, L., Reinecke, H., and Murry, C.E. (2011). Growth of engineered human myocardium with mechanical loading and vascular coculture. Circ. Res. *109*, 47–59.

van den Berg, C.W., Okawa, S., Chuva de Sousa Lopes, S.M., van Iperen, L., Passier, R., Braam, S.R., Tertoolen, L.G., del Sol, A., Davis, R.P., and Mummery, C.L. (2015). Transcriptome of human foetal heart compared with cardiomyocytes from pluripotent stem cells. Development *142*, 3231–3238.

Vreeker, A., van Stuijvenberg, L., Hund, T.J., Mohler, P.J., Nikkels, P.G., and van Veen, T.A. (2014). Assembly of the cardiac intercalated disk during pre- and postnatal development of the human heart. PLoS One *9*, e94722.

Yang, X., Pabon, L., and Murry, C.E. (2014a). Engineering adolescence: maturation of human pluripotent stem cell-derived cardiomyocytes. Circ. Res. *114*, 511–523.

Yang, X., Rodriguez, M., Pabon, L., Fischer, K.A., Reinecke, H., Regnier, M., Sniadecki, N.J., Ruohola-Baker, H., and Murry, C.E. (2014b). Tri-iodo-l-thyronine promotes the maturation of human cardiomyocytes derived from induced pluripotent stem cells. J. Mol. Cell Cardiol. *72*, 296–304.

Zhu, R., Blazeski, A., Poon, E., Costa, K.D., Tung, L., and Boheler, K.R. (2014). Physical developmental cues for the maturation of human pluripotent stem cell-derived cardiomyocytes. Stem Cell Res. Ther. *5*, 117.

Stem Cell Reports, Volume *8*

Supplemental Information

In Vivo Maturation of Human Induced Pluripotent Stem Cell-Derived Cardiomyocytes in Neonatal and Adult Rat Hearts

Shin Kadota, Lil Pabon, Hans Reinecke, and Charles E. Murry

Figure S1. Related to Figure 1

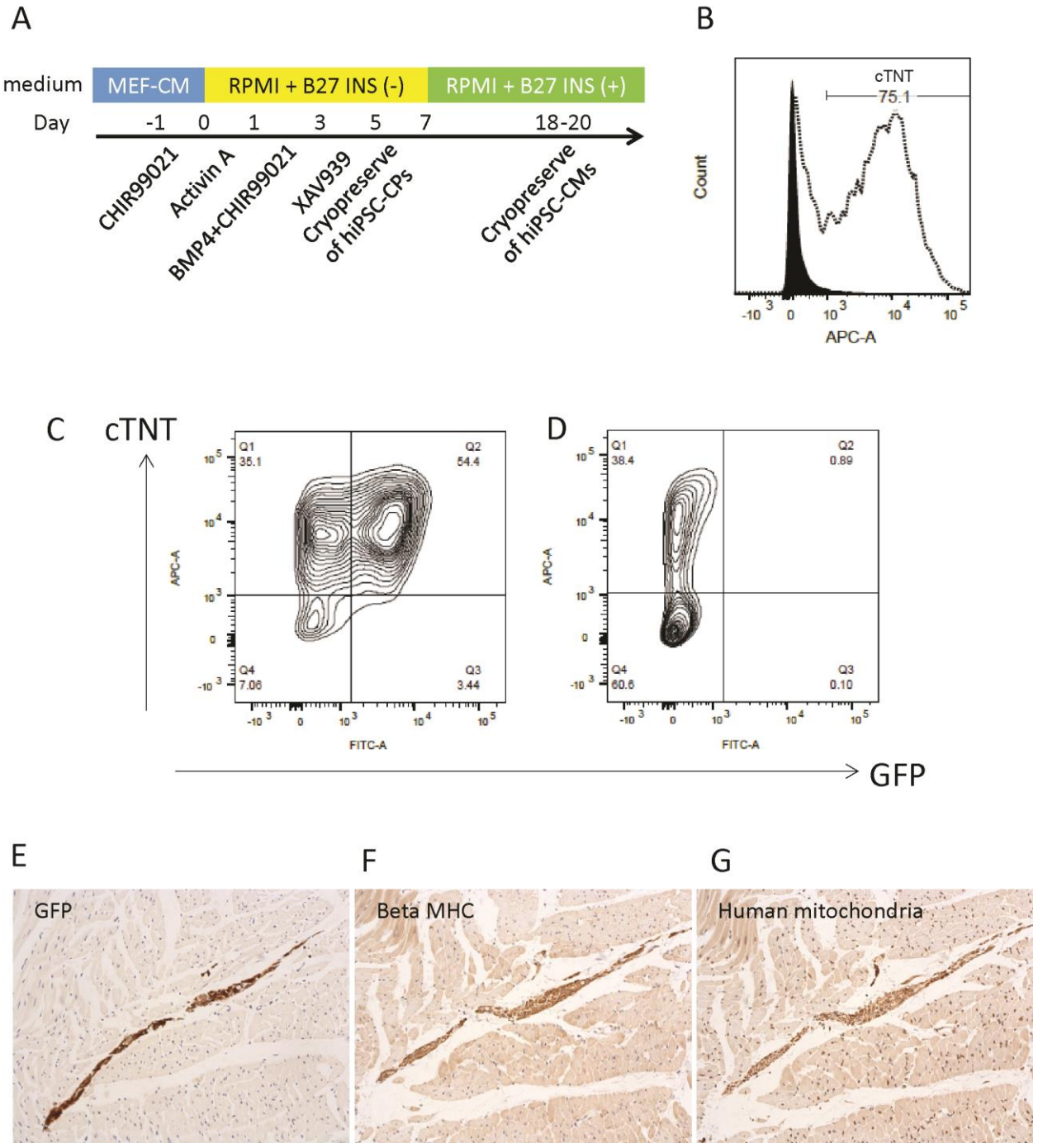

Figure S2. Related to Figure 2

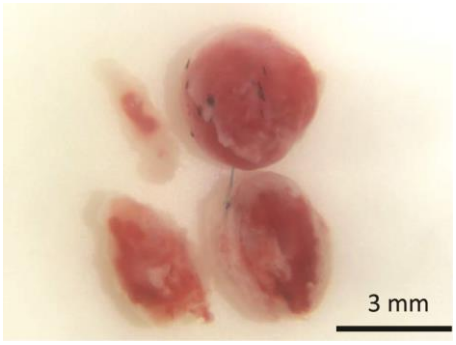

Figure S3. Related to Figure 3

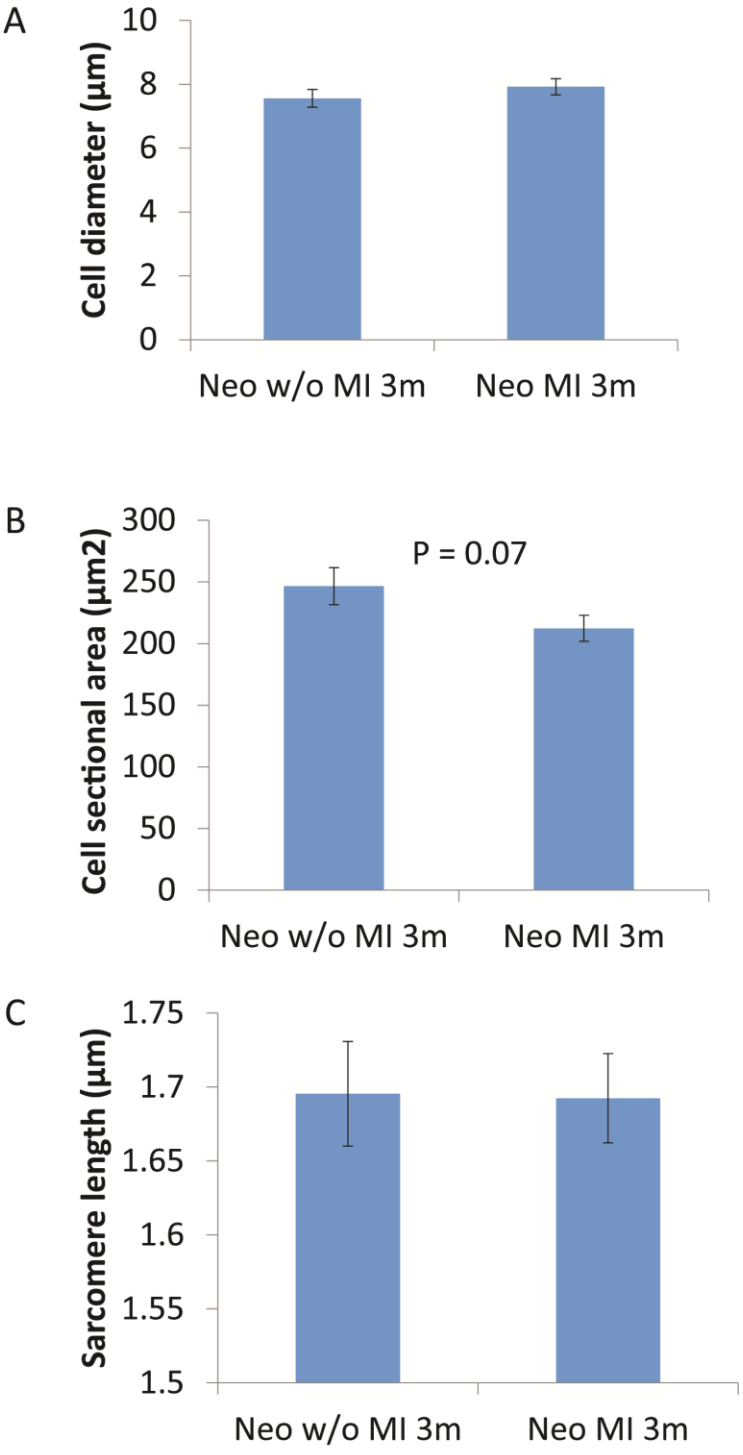

Figure S4. Related to Figure 4

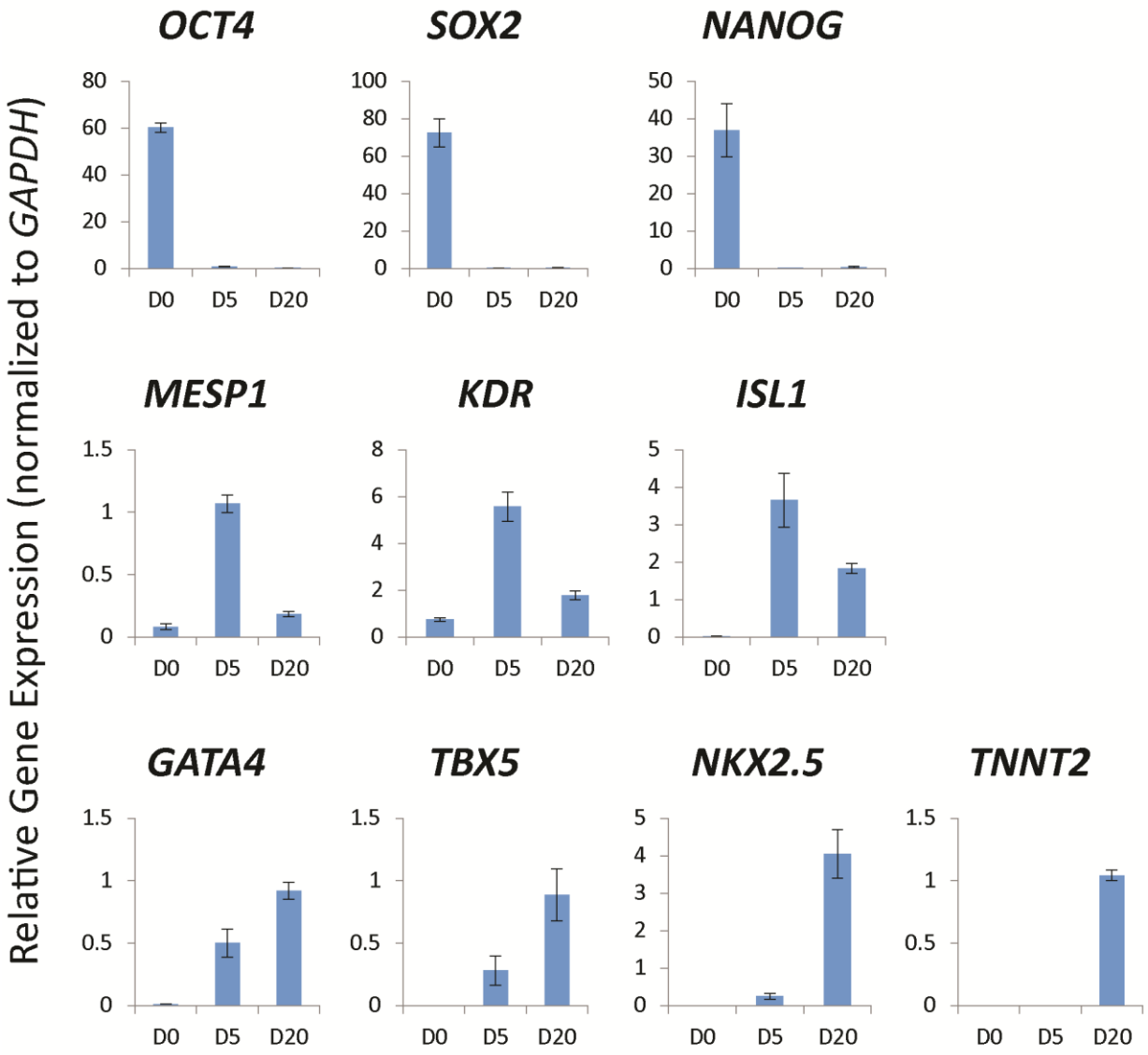

Figure S5. Related to Figure 5

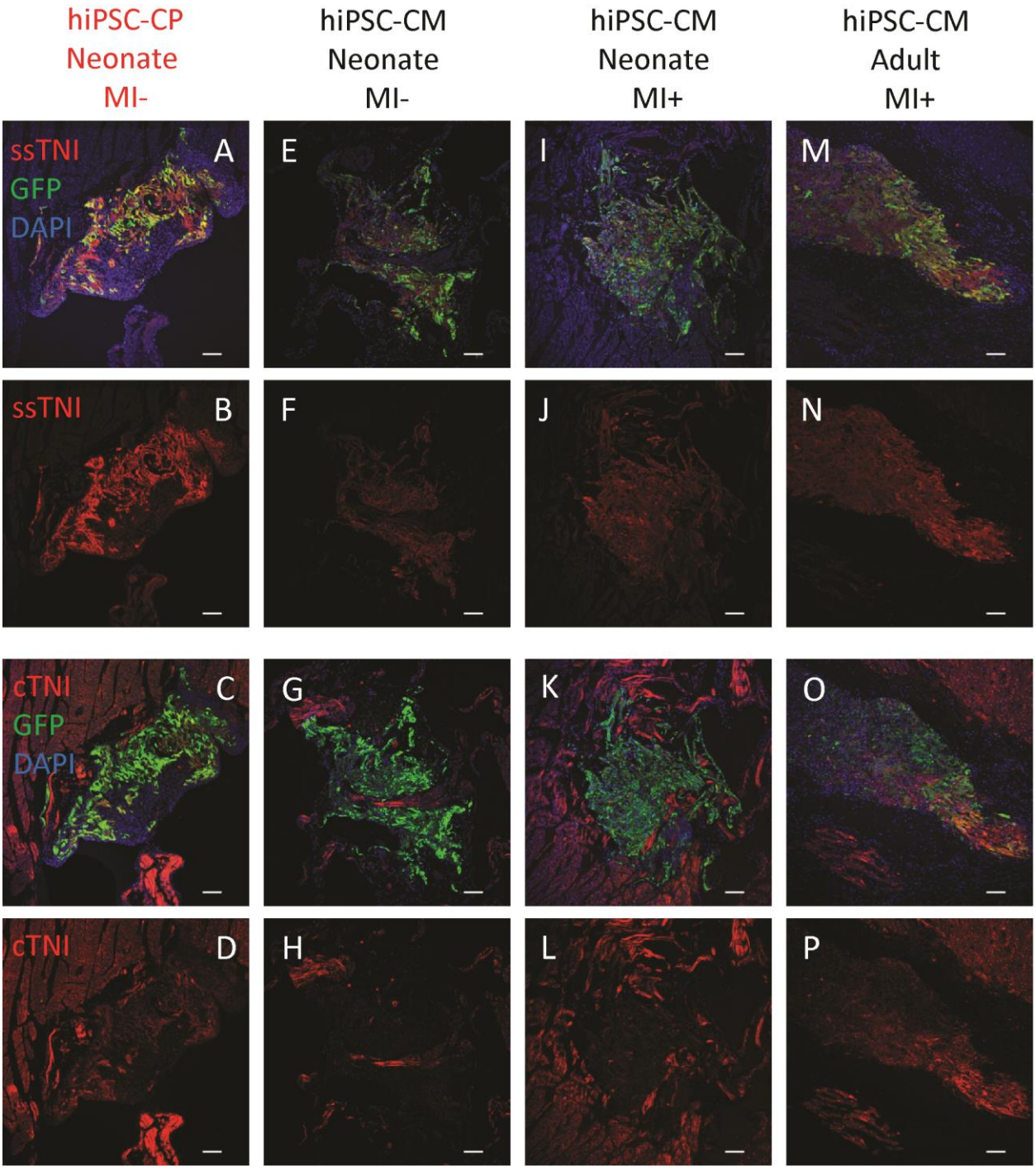

Supplemental figure legends

Figure S1. Differentiation protocol, flow cytometry and immunostaining for detection of hiPSC-CMs.

A: Scheme of monolayer based direct-differentiation protocol. We harvested and cryopreserved hiPSC-derived cardiac progenitors (hiPSC-CPs) and cardiomyocytes (hiPSC-CMs) at day 5 and 18-20 after differentiation, respectively. MEF-CM = mouse embryonic fibroblast-conditioned medium. INS = insulin. **B**: FACS analysis of day 20 hiPSC-derived cells stained cardiac troponin T (cTNT). Black population is negative control which was stained with isotype antibody. **C-D**: Flow cytometry for differentiated cells at day 20 of 253G1-GCaMP3 which were used in this study (**C**) and wild type 253G1 (**D**) stained cTNT. **E-G**: Serial sections of engrafted hPSC-CMs after 84 days of cell injection to uninjured neonatal rat hearts with GFP (**E**), beta-myosin heavy chain (MHC, **F**) and human mitochondria (**G**) staining.

Figure S2. TTC staining.

Representative image of TTC staining of injured heart at 3 days after MI of neonatal rat.

Figure S3. Comparison of hiPSC-CMs in neonatal rat hearts with and without injury.

Comparisons of cell diameter (**A**), cell sectional area (**B**), and sarcomere length (**C**) of engrafted hiPSC-CMs in neonatal rat with and without MI at 3 months after cell injection. N=40 (**A-C**). Data are mean ± SEM.

Figure S4. qRT-PCR.

Horizontal axis shows days after cardiac differentiation. Cardiac mesoderm markers (*MESP1*, *KDR* and *ISL1*) were highly and early cardiac development makers (*GATA4* and T*BX5*) moderately upregulated in day-5 differentiated hiPSC-CPs, although they did neither expressed pluripotent markers (*OCT4*, *SOX2* and *NONOG*), nor cardiac markers (*NKX2.5* and *TNNT2*). N=3 biological replicates. Data are mean ± SEM.

Figure S5. Immunostaining of Troponin I.

Comparison of hiPSC derivatives engrafted in rat hearts after 3 months of cell transplantation with slow skeletal troponin I (ssTNI) and cardiac TnI (cTNI) staining. Representative graft of hiPSC-CP transplantation to neonatal rat without MI (**A-D**), hiPSC-CM transplantation to neonatal rat without MI (**E-H**), neonatal rat with MI (**I-L**), and

adult rat with MI (**M-P**). Scale bar = 100 μm.

Supplemental Tables

Table S1. Antibodies for immunostaining.

Antigen	Antibody type	Company	Catalog number or clone	Concentration	Antigen retrieval
GFP	Rabbit polyclonal	Novus	NB600-308	1:1000	
GFP	Goat polyclonal	Novus	NB100-1770	1:1000	
Beta-Myosin Heavy Chain	Mouse monoclonal	Developmental Studies Hybridoma Bank	A4.951	1:10	Citrate HIER
Human mitochondria	Mouse monoclonal	Millipore	MAB1273	1:100	EDTA HIER
Troponin I type 1 (slow skeletal)	Rabbit polyclonal	Novus	NBP1-56641	1:200	Citrate HIER
Cardiac Troponin I	Rabbit polyclonal	Abcam	ab47003	1:200	Citrate HIER
Alpha-actinin	Mouse monoclonal	Sigma-Aldrich	A7811	1:500	Tris-EDTA HIER
Caveolin 3	Rabbit polyclonal	Abcam	ab2912	1:500	Tris-EDTA HIER
N-cadherin	Mouse monoclonal	Sigma-Aldrich	GC-4	1:200	Citrate HIER
Connexin 43	Rabbit polyclonal	Sigma-Aldrich	C6219	1:200	Citrate HIER
Wheat Germ Agglutinin, Alexa Fluor 594 Conjugate		Thermo Fisher	W11262	1:200	

HIER: Heat-induced epitope retrieval

Table S2. Primers for qRT-PCR.

	Forward primer	**Reverse primer**
OCT4	GGGTTCTATTTGGGAAGGTAT	TTCATTGTTGTCAGCTTCCT
SOX2	GCCGAGTGGAAACTTTTGTCG	GGCAGCGTGTACTTATCCTTCT
NANOG	TTTGTGGGCCTGAAGAAAACT	AGGGCTGTCCTGAATAAGCAG
ISL1	ATTTCCCTATGTGTTGGTTGC	CGTTCTTGCTGAAGCCGATG
KDR	GCACAAAGTGACACGTTGAGAT	AGTGATCGGAAATGACACTGGA
MESP1	TCGAAGTGGTTCCTTGGCAGAC	CCTCCTGCTTGCCTCAAAGTGTC
GATA4	ACACCCCAATCTCGATATGTTTG	GTTGCACAGATAGTGACCCGT
TBX5	GAACCACAAGATCACGCAATTA	ACACCATTCTCACACTGGTAT
NKX2.5	ACCCTGAGTCCCCTGGATTT	TCACTCATTGCACGCTGCAT
TNNT2	TTCACCAAAGATCTGCTCCTCGCT	TTATTACTGGTGTGGAGTGGGTGTGG
GAPDH	ATGGAAATCCCATCACCATCTT	CGCCCCACTTGATTTTGG